High Resolution Scintillating Screens for Measurements of few Micrometer Beams

Gero Kube
DESY (Hamburg)

- Introduction
- Spatial Resolution for different Scintillators
- Influence on Observation Geometry
- Measurement of few Micrometer Beam
- Scintillator Non-Linearity
- (Comments on Digital Camera Systems)

OTR Transverse Beam Profiling

- Optical Transition Radiation (OTR) for beam diagnostics
  - backward OTR: reflection of virtual photons

    → instantaneous process
  - single shot measurement
  - full transverse (2D) profile information

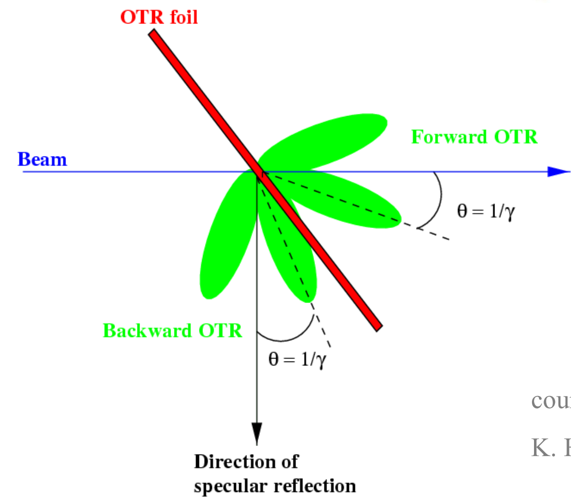

courtesy:
K. Honkavaara (DESY)

- Coherent OTR observation at LCLS (SLAC)

  R. Akre et al., Phys. Rev. ST Accel. Beams **11** (2008) 030703

  H. Loos et al., Proc. FEL 2008, Gyeongju, Korea, p.485.

  - OTR 12

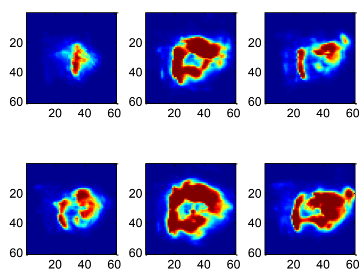

  - OTR 22

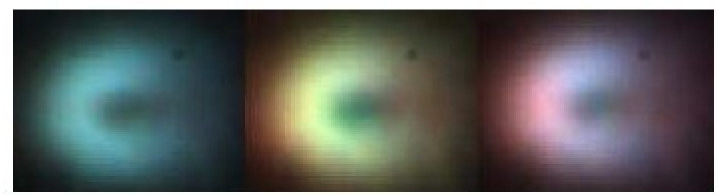

  - strong shot-to-shot fluctuations
  - doughnut structure
  - change of spectral contents

→ measured spot is no beam image!

- interpretation of coherent formation in terms of "Microbunching Instability"

  E.L. Saldin et al., NIM **A483** (2002) 516 Z. Huang and K. Kim, Phys. Rev. ST Accel. Beams **5** (2002) 074401

- alternative schemes for beam profile diagnostics
  - stochastic radiation emission (destruction of coherence) → multi-stage emission process

Scintillation Light Generation

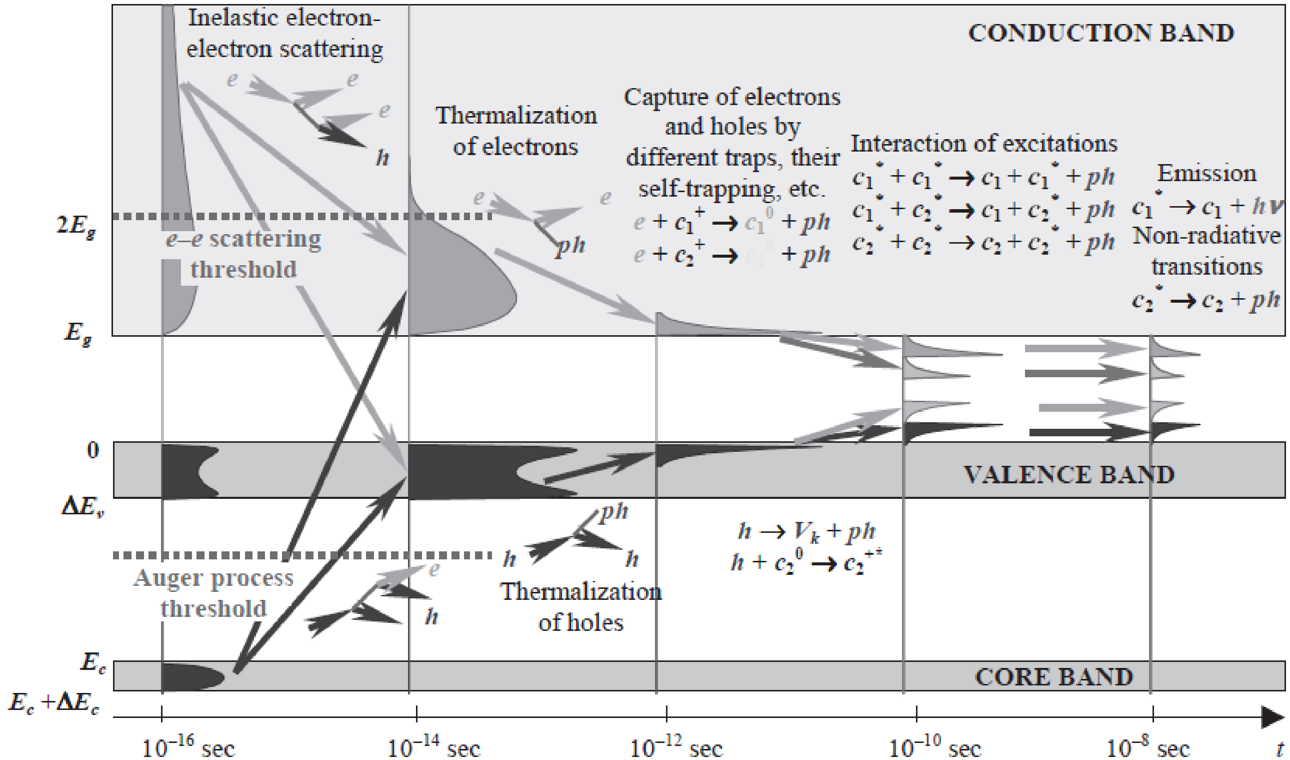

A.N. Vasil'ev, Proc. SCINT'99, Moscow (Russia), 1999, p.43

- multi-stage process
  - energy conversion → generation of "hot" electronic excitations
  - thermalization → phonon emission: transform E_{kin} of excitations in heat
  - localization → excitation interaction with defects/impurities
  - transfer to luminescent centers → migration of relaxed excitons
  - radiative relaxation → emission of scintillation light

Scintillators for Beam Diagnostics

- review of scintillators for beam profile measurements
  - phosphor screens: **P11** (ZnS:Ag), **P20** ([Zn,Cd]S:Ag), **P43** (Gd_2O_2S:Tb), …
    → decay times O(ms), resolution limited by grain size
  - ceramic screens: Chromox (Al_2O_3:Cr)
    → higher radiation hardness, better thermo-mechanical properties, lower light yield
  - inorganic scintillators: CsI:Tl, **YAG:Ce** → „high resolution monitor" W.S. Graves et al., Proc. PAC'97 (1997) 1993
    → better resolution, higher light yield than Chromox

  ➡ status in 2003: R. Jung et al., Proc. DIPAC2003, IT03, p. 10

- scintillators for beam diagnostics
  - heavy ion accelerators → standard for beam profile measurements (typically ceramic screens)
  - electron accelerators → powders/inorganic scintillators used for gun diagnostics (OTR intensity to low)
  - DIPAC invited talk 2007 → E. Bravin, „High Resolution Transverse Profile Measurement", Proc. DIPAC2007, p.1
    → scintillators for high resolution even not covered…

- COTR problem at LCLS in 2008
  - return to scintillator based beam profile diagnostics @ FELs
    → Workshop on „*Scintillating Screen Applications in Beam Diagnostics*" @ GSI, February 2011

  B. Walasek-Höhne, C. Andre, P. Forck, E. Gütlich, G. Kube, P. Lecoq, and A. Reiter, IEEE Trans. Nucl. Sci. **59** (2012) 2307

Scintillators for Beam Diagnostics (2)

- requirements for beam diagnostics application
  - high spatial resolution → material property
  - high sensitivity → high stopping power, material property
  - good linearity → short decay time, material property
  - radiation resistant → inorganic scintillators widely used in high energy physics, dosimetry,…

unknown

- minimum distortion of optical path
  - light generated inside scintillator has to cross boundary

    → refractive index n

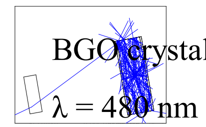

  - inorganic scintillotors: **large *n***

    → large contribution of total reflection

    → **influence on observation geometry**

- since beginning of 20th century: development of new inorganic scintillator materials
  - high energy physics (calorimtery), medical physics (PET imaging, ...)

    → BGO, YAP, LuAG, LuAP, YAP, LSO, LYSO, GGAG, $LaCl_3$, $LaBr_3$, SrI_2, …

➡ interest in testing new materials for beam diagnostics (→ why only YAG:Ce ?)

Test Experiments

- Mainz Microtron MAMI

Institute of Nuclear Physics, University of Mainz (Germany)

3 cascaded Racetrack Microtrons: **E_{max} = 855 MeV**
double-sided Microtron (HDSM): **E_{max} = 1.5 GeV**
100 % duty cycle
polarized electron beam (~ 80%)

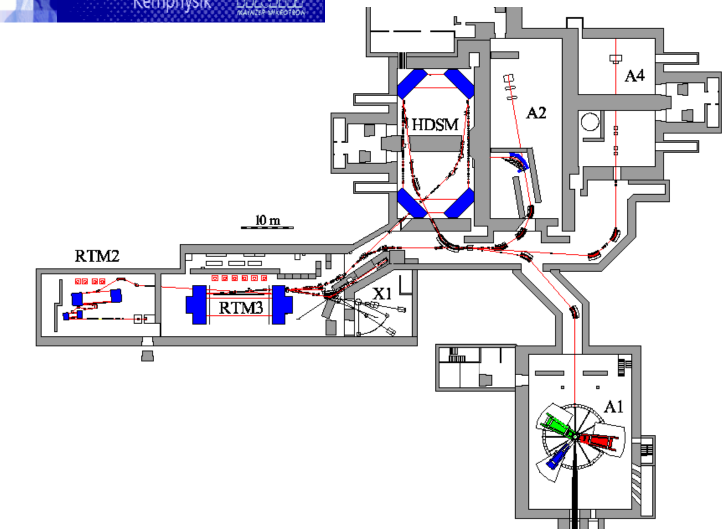

- test experiments in X1 beamline
  - target chamber with goniometric stages
  - observation geometry

-22.5° w.r.t. beam axis

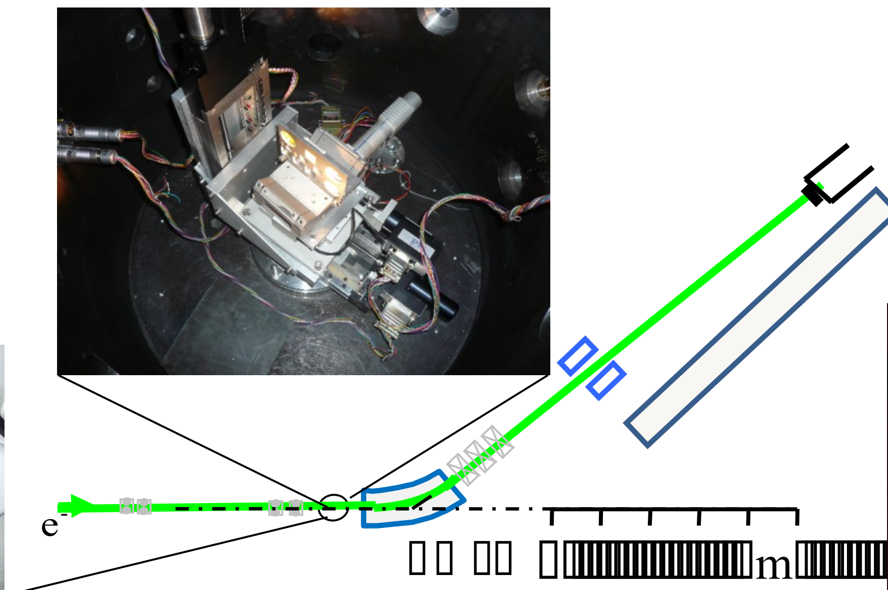

- target holder

Spatial Resolution

- experiment 2009
  - BGO 0.5 mm
  - PWO 0.3 mm
  - LYSO:Ce 0.8 mm, 0.5 mm (Prelude 420)
  - YAG:Ce 1.0 mm, 0.2 mm, powder
  - Al_2O_3 1.0 mm (ceramic)
- experiment 2011
  - BGO 0.3 mm
  - LYSO:Ce 0.3 mm (Prelude 420, CRY-19)
  - YAG:Ce 0.3 mm
  - LuAG:Ce 0.3 mm
  - YSO:Ce (?) 0.3mm (CRY-18)

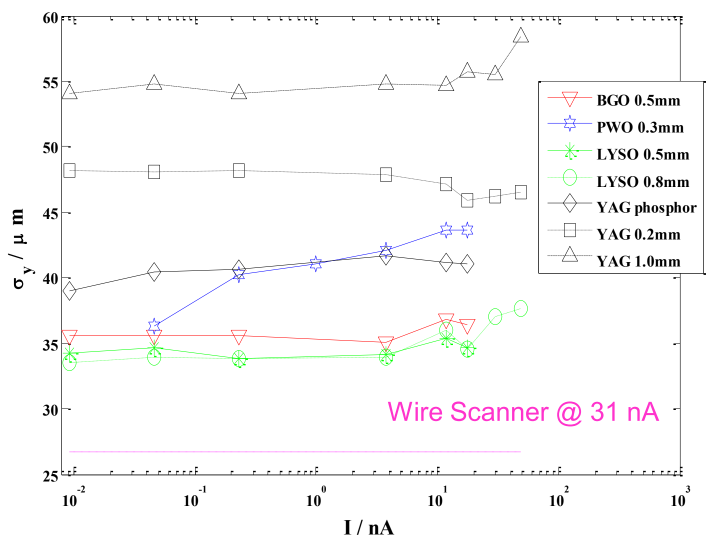

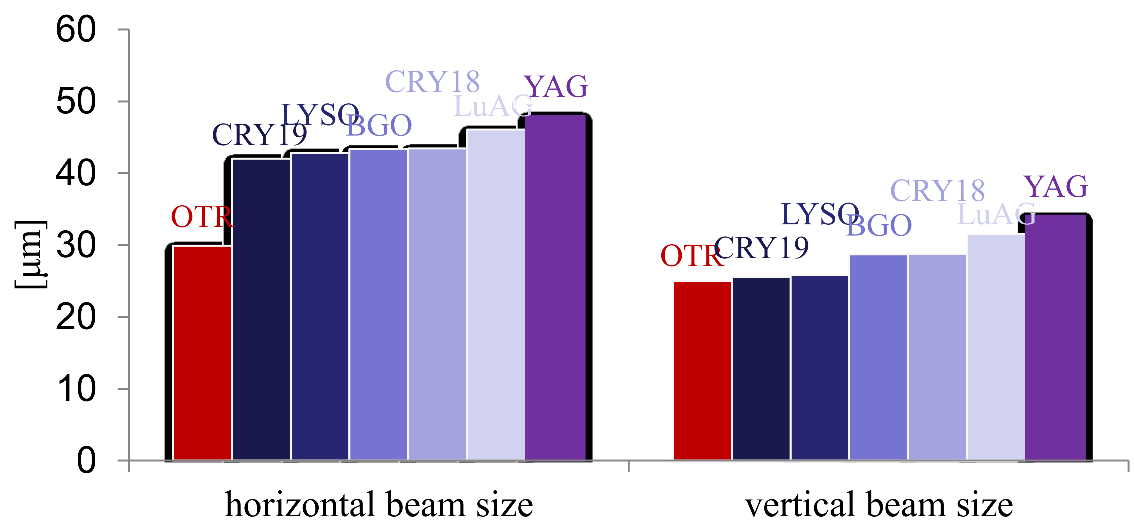

G. Kube et al., Proc. IPAC'10, Kyoto (Japan), 2010, p.906

G. Kube et al., Proc. IPAC'12, New Orleans (USA), 2012, p.2119

→ **LYSO:Ce best spatial resolution**

Observation Geometry

- beam diagnostics

  → popular OTR-like observation geometry:

45°tilt of screen

observation under 90°

→ **turns out to be bad!**

- scintillator tilt versus beam axis

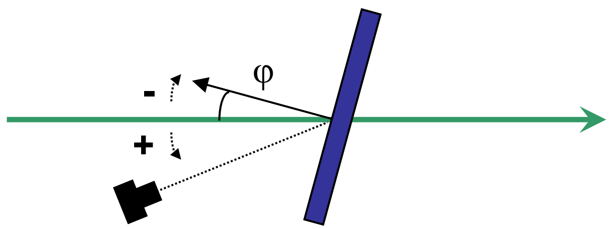

BGO crystal

micro-focused beam

I = 3.8 nA

- measured beam spots

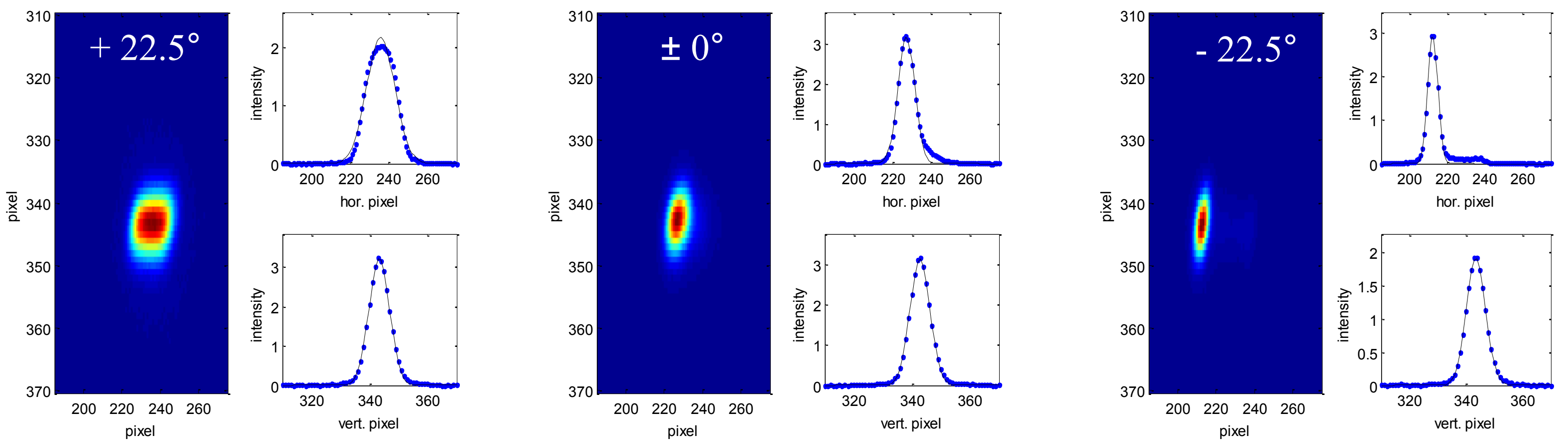

Comparison

- light propagation in scintillator
  - simple ZEMAX model → light generated by line source, scintillator characterized by n

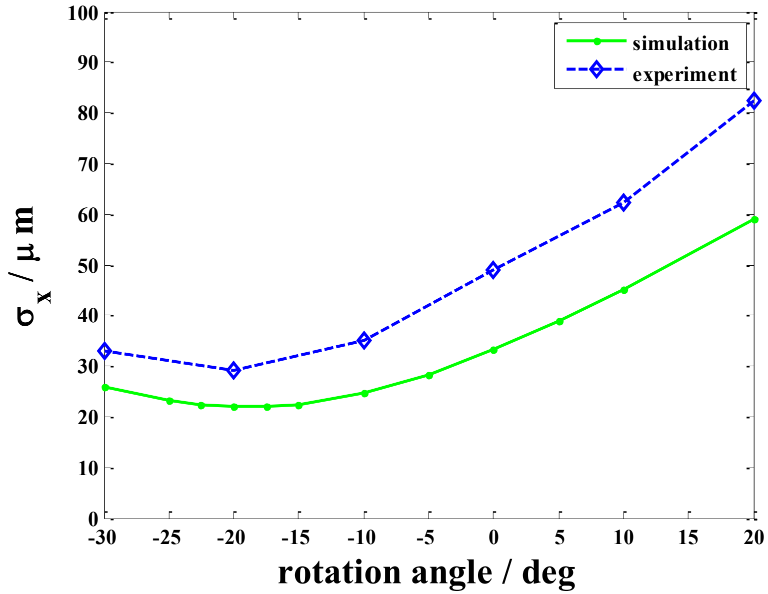

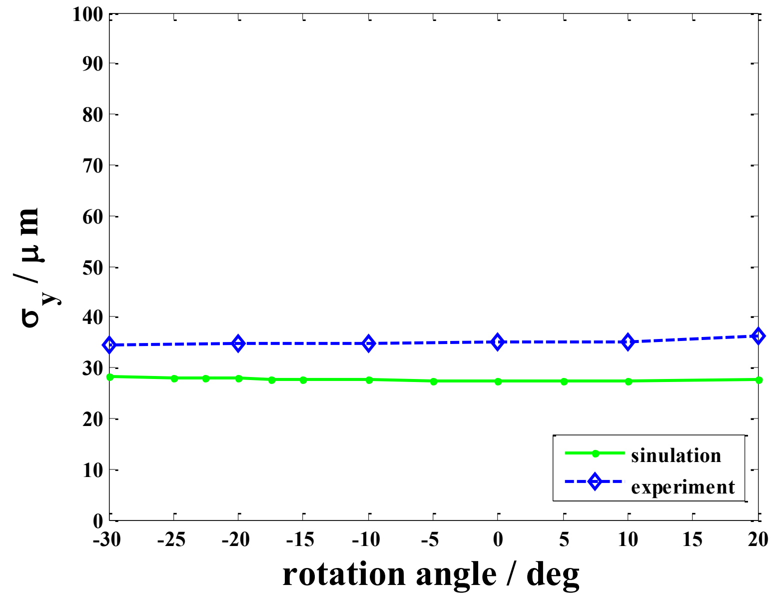

- satisfactory agreement between simulation and measurement

  → simulation reproduces observed trend in beam size

- measured beam size systematically larger than simulated one

  → effect of scintillator material properties not included in calculation → increase in PSF

G. Kube, C. Behrens, and W. Lauth, Proc. IPAC 2010, Kyoto, Japan, p.906.

Observation Geometry Influence

- comparison observation geometry

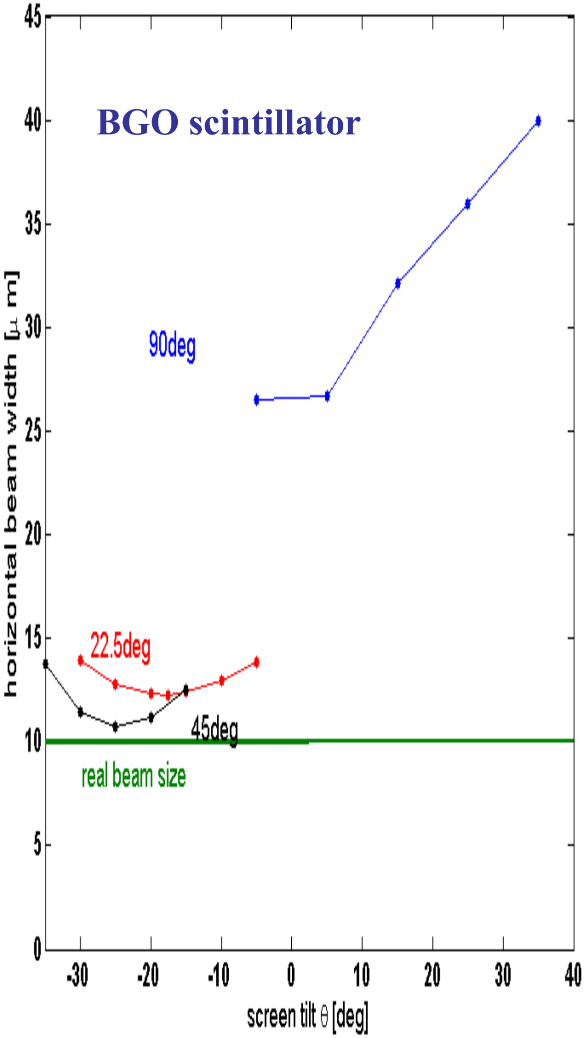

Top-view

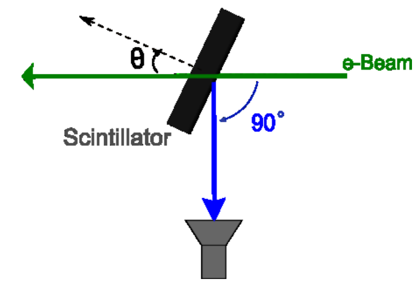

OTR screen

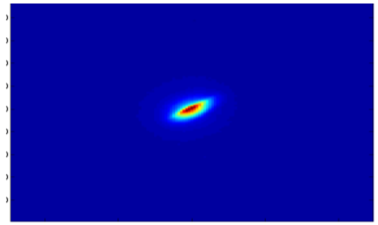

BGO screen, θ = 15°

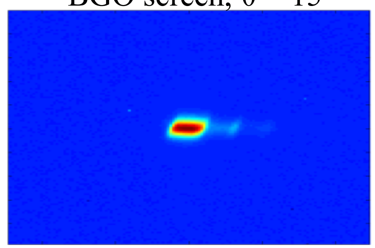

BGO screen, θ = 45°

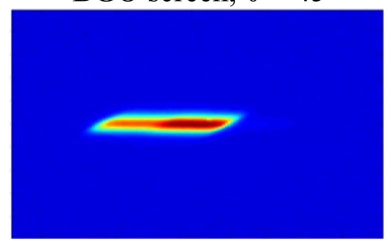

BGO screen, θ = 55°

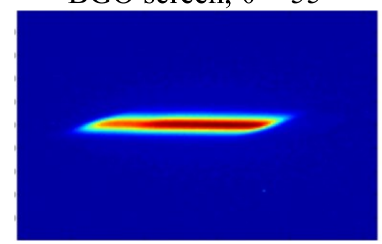

OTR screen

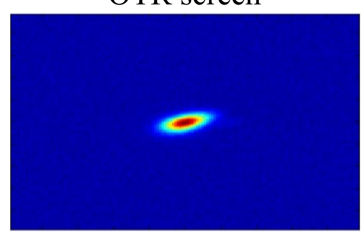

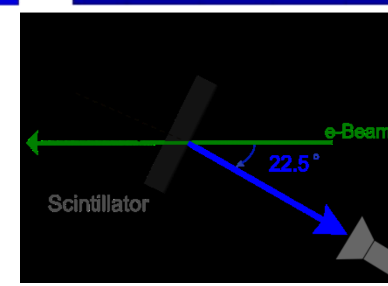

BGO screen, θ = -25°

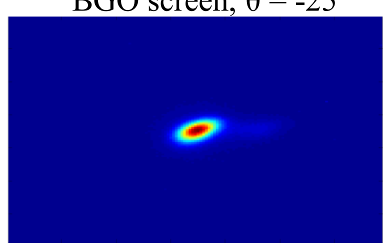

BGO screen, θ = 0°

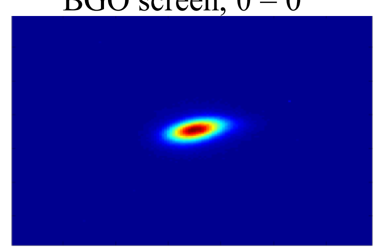

BGO screen, θ = +25°

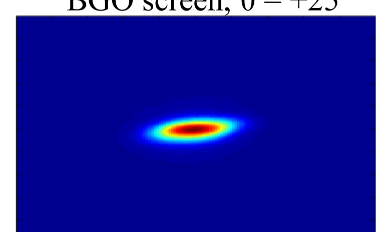

Exploring the Resolution Limits

- micrometer beam size experiment at MAMI

G. Kube, S. Bajt, A.P. Potylitsyn, L.G. Sukhikh, A.V. Vukolov, I.A. Artyukov, W. Lauth, Proc. IBIC2015, Melbourne, Australia, p.330

  - experimental scheme

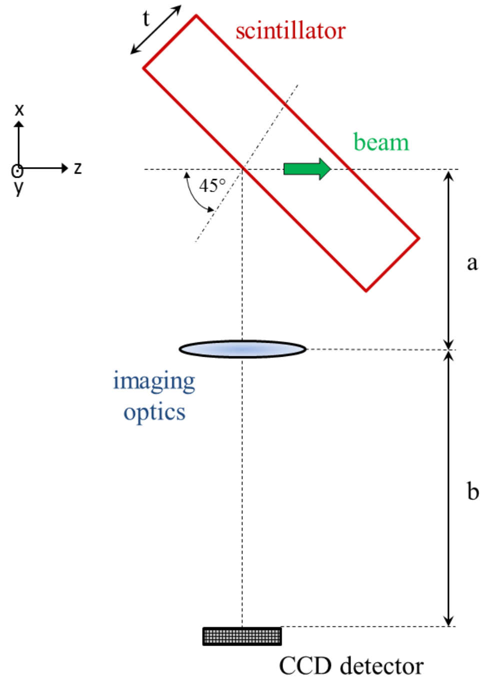

a = 27.54 mm

b = 1155.46 mm

→ M = 41.95

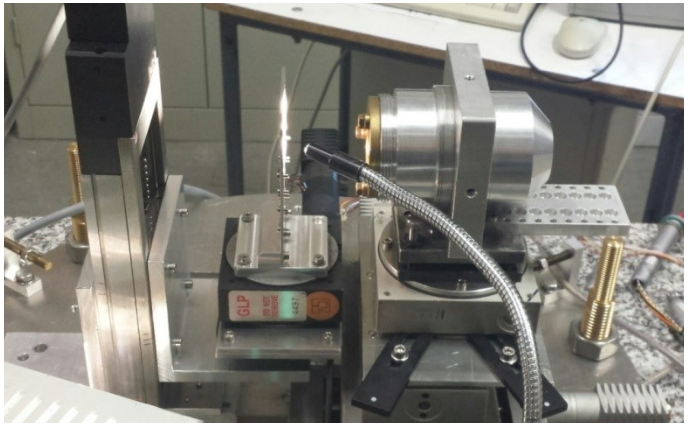

Target: LYSO scintillator ($Lu_{2(1-x)}Y_{2x}SiO_5$:Ce)

thickness t = 200 μm

supplier: *OmegaPiezo*

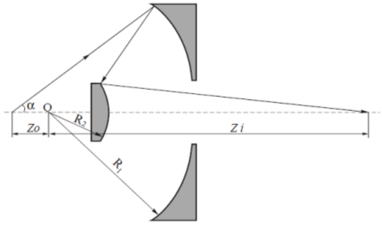

Schwarzschild Objective:

→ 2 concentric spherical mirrors

→ aplanatic (corrected for spherical aberrations)

f = 26.90 mm

NA = 0.19 (nominal)

Micrometer Beam Size Measurement

- measured beam image

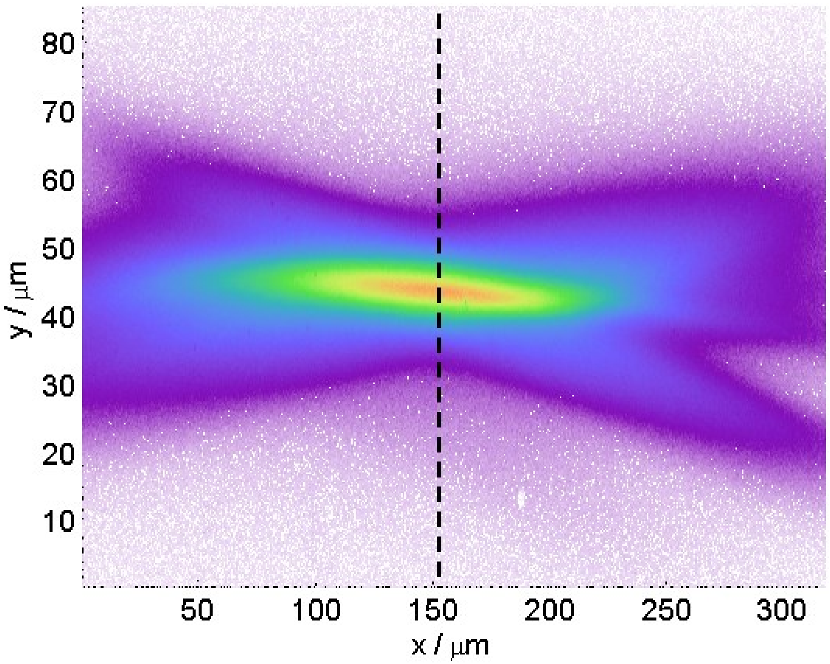

- horizontal beam profile
  - → affected by OTR-like 90° observation geometry
- vertical beam profile
  - → affected by depth-of-focus

➡ restriction: analysis only along vertical cut

- **analysis**: scintillator model in Zemax©
  - → light emission from single electron represented by line source in LYSO crystal with isotropic light emission
  - → scintillator properties described by n(λ)
  - → Schwarzschild objective replaced by paraxial lens with same f and appropriate NA
  - → non-sequential ray tracing for 10^8 rays at LYSO peak emission wavelength λ = 420 nm
    - → single particle resolution function (SPF)
  - → SPF convolution with 2D-Gaussian (beam profile)
  - → vertical cut and comparison

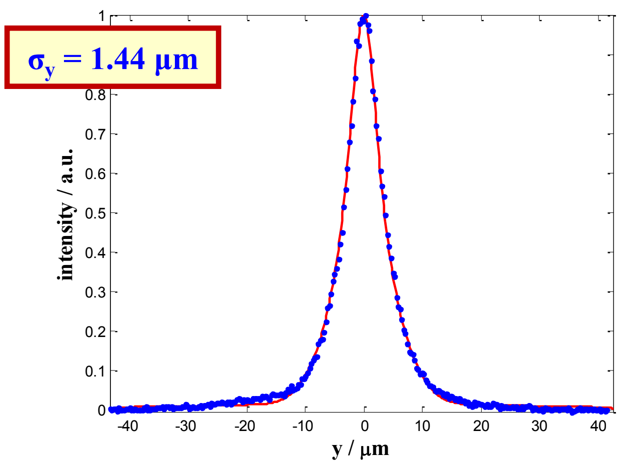

Sensitivity - Parameter Influence

- beam size

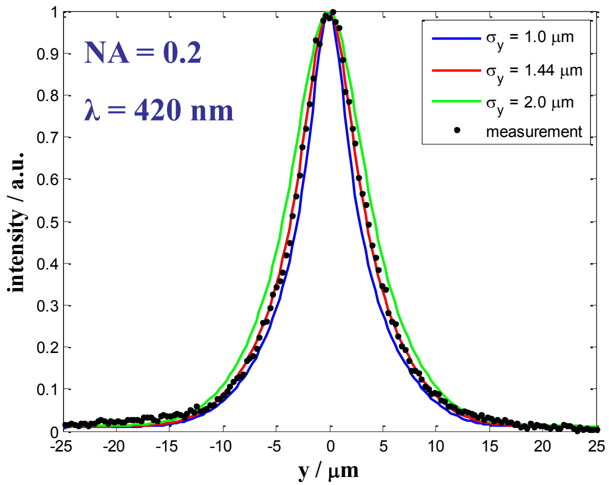

  - affects central part of distribution

- numerical aperture

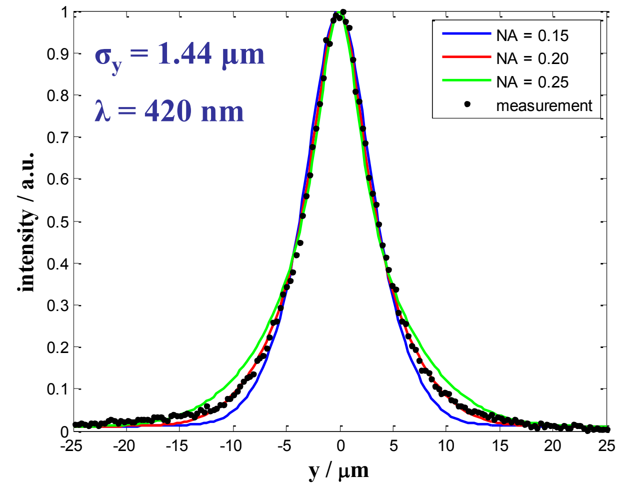

  - affects tails of distribution

- resolution improvement

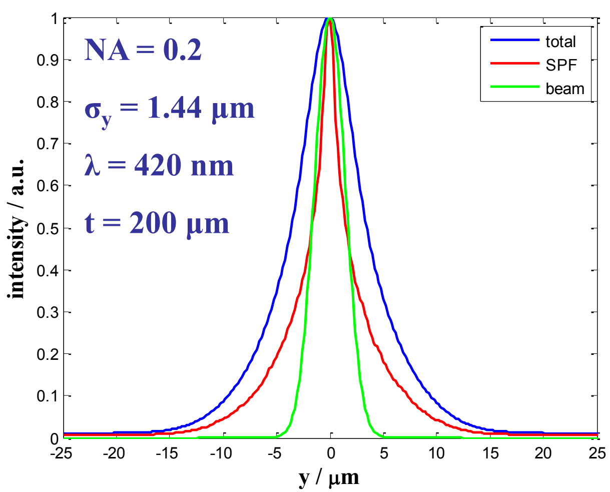

  - individual contributions

reduce t

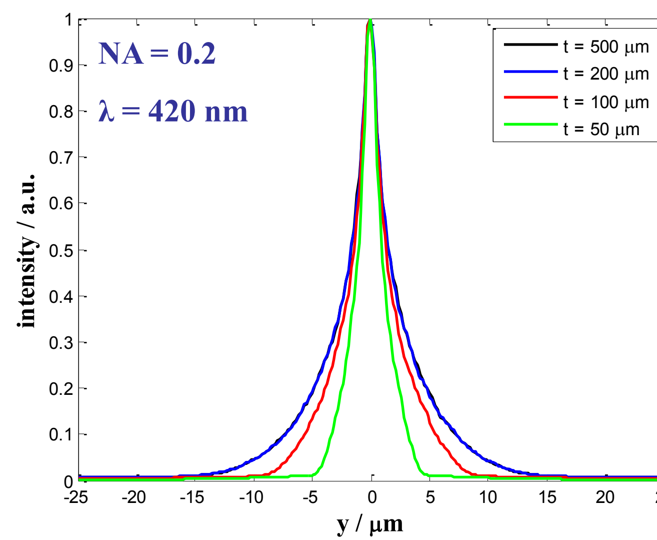

Conclusion and Outlook

- search for high resolution scintillator materials
  - suitable candidate: LYSO:Ce
- influence on observation geometry
  - considerable influence on spatial resolution
  - basic understanding in frame of geometrical light propagation
- micrometer beam size measurements
  - micrometer beam size measured with 200 μm thick LYSO:Ce scintillator
  - analysis requires knowledge of Single Particle Function (SPF)
  - better sensitivity for thinner crystals
- XFEL screen monitors: perturbed beam profiles
  - measured emittance values larger than expected
  - assumption: scintillator effect
    - → caused by high *ionization track denisty* due to *primary beam density*
    - → quenching of excitation centers
  - search for better scintillator materials
    - → next weekend : beam test at XFEL

e/γ-Response of Scintillators

- scintillators used for γ-ray beam profile measurements
  - X-ray converter for CCDs → e.g. for pinhole camera

➡ difference in scintillator response between ***electrons*** and ***photons*** ?

- electron response
  - collisional stopping power
    - → several small interactions
    - → mainly with outer shell electrons

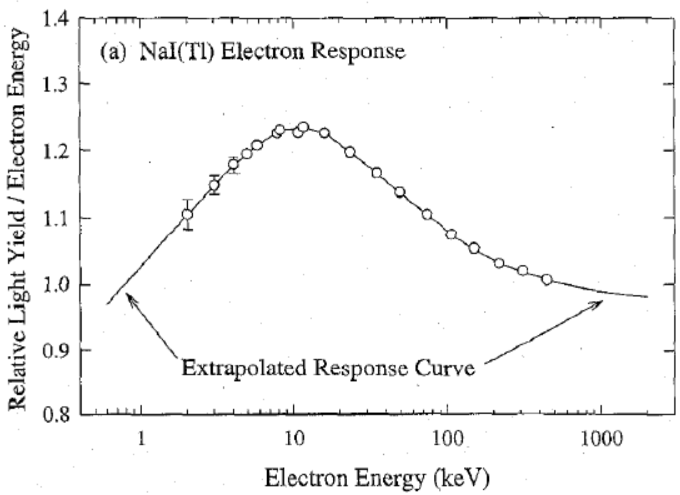

- photon response
  - photo effect
    - → single interaction, predominantly with inner shells
    - → complex cascade structure

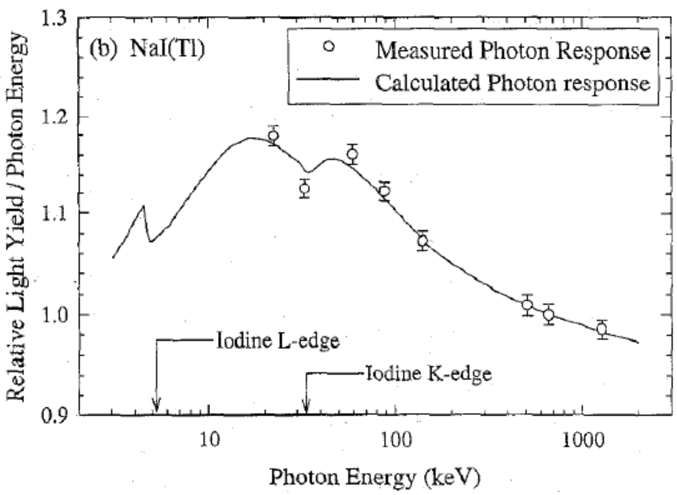

B.D. Rooney and J.D. Valentine, IEEE Trans. Nucl. Sci. **44** (1997) 509

- smooth electron response
- photon response with substructure

Comments on Digital Camera Systems for Beam Diagnostics Applications

Gero Kube
DESY (Hamburg)

- Charge-Coupled Devices (CCD)
- CMOS Imaging Sensor (CIS)
- Sensor Performance Study

➡ only Cameras for Machine Vision

CCD Working Principle

- image generation with CCD: 4 stage process
  - charge generation
  - charge collection
  - charge transfer
  - charge measurement

- charge generation & collection: fundamental light-sensing unit
  - metal oxide semiconductor (**MOS**) capacitor
  - operated as a photodiode and storage device
  - photo effect: conversion of incoming photons into charge
  - reverse bias operation

    → electrons migrate to area underneath positively charged gate electrode (well capacity: 1000-2000 $e^-/\mu m^2$)

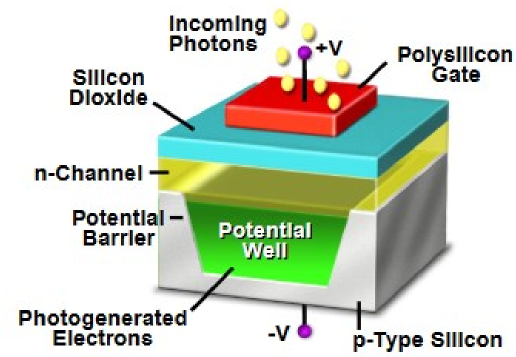

https://www.microscopyu.com

- charge transfer
  - CCD sense element (pixel) structure

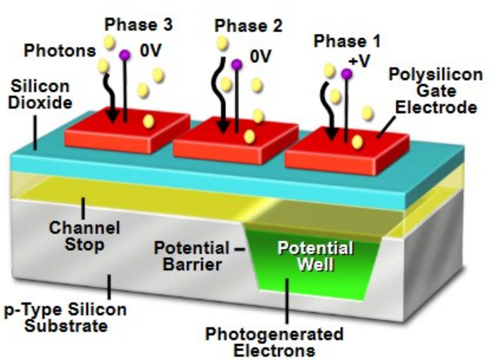

https://www.microscopyu.com

→ line array of pixels forms transfer register

→ ***transfer*** of charge packets ***according to voltage*** applied to the gate terminals

→ requires overlap of depletion region in transfer direction

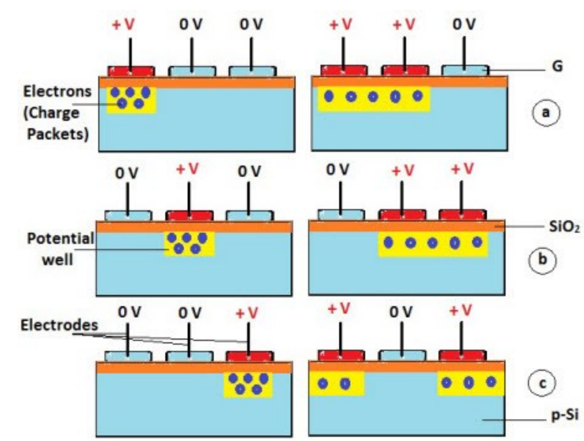

https://www.elprocus.com/know-about-the-working-principle-of-charge-coupled-device/

CCD Working Principle (2)

- charge transfer (cntd.)
  - CCD array is series of column registers
    - → charge kept within rows by channel stops
  - end of each column: horizontal shift register
    - → collects a line at a time
    - → transports charge packets in serial fashion to output amplifier
    - → entire horizontal register has to be clocked out before next line enters
    - → requires separate horizontal (fast) / vertical (slow) clocks
  - gate voltages ~8…15 V required for creation of depletion wells
    - → rapidly turn on/off for charge transport → high power consumption

water bucket analogy:

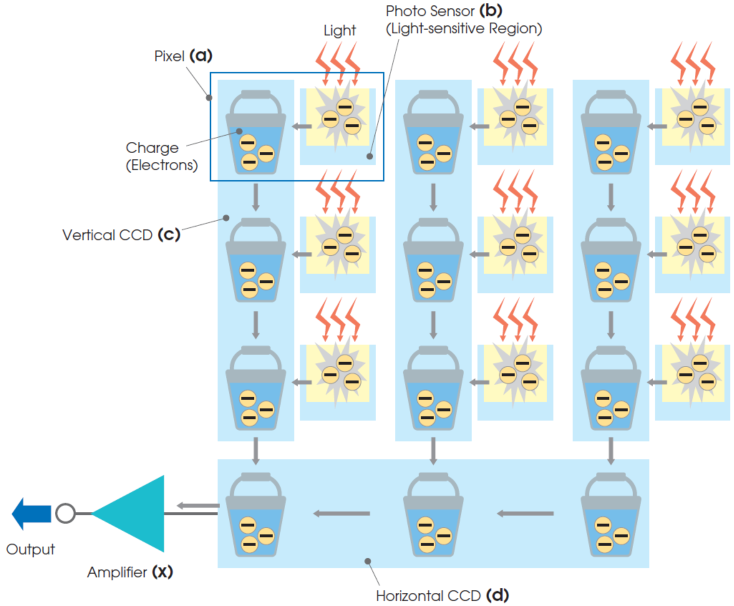

www.sony.com/professional

- charge measurement

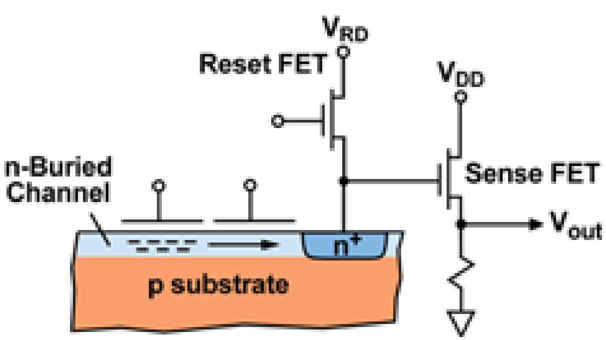

- n^+: ***floating diffusion*** or ***sense node***
  - → region in active silicon (diffusion) region, electrically isolated
  - → potential determined by the amount of stored charge and capacitance
- Sense FET: ***source follower*** configuration (impedance transformation)
  - → buffers poor voltage source (high R_i) into nearly ideal one (low R_i), A~1
- Correlated Double Sampling (CDS): measure after reset & charge dump + subtract
  - → reduce signal fluctuations

https://www.ll.mit.edu/mission/electronics/ait/hisensitivityimage.html

CMOS Working Principle

- CMOS : Complementary Metal-Oxide-Semiconductor
  - well established technology for constructing integrated circuits
    - → evolved to smaller circuit sizes → lower power consumption
- CMOS Imaging Sensor (CIS): active pixel sensor most popular design
  - photodiode and readout amplifier incorporated into each pixel
    - → CIS contains analogue and digital components
  - accumulated ***charge*** converted into ***voltage*** inside pixel
  - voltage conversion similar to CCD
    - → source follower & voltage signal amplification (otherwise too small to be transferred)
  - if pixel selected
    - → pixel readout via external readout circuitry

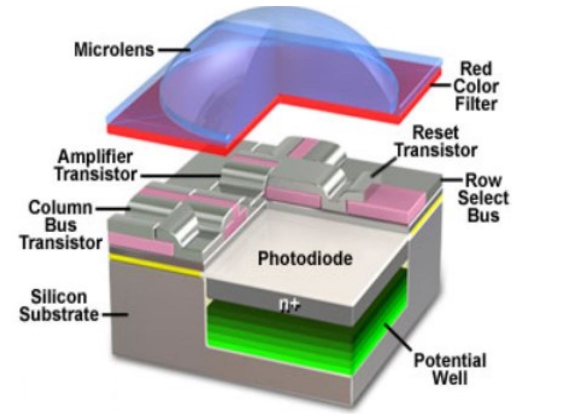

https://www.olympus-lifescience.com/en/microscope-resource/primer/

- pixel architecture
  - 3T(ransistors): Reset, Source Follower, Select
    - → small pixels, for consumer market (cell phone,…)
    - → ***rolling shutter*** (problems with moving object)
  - 4T: …+ Transfer Gate TX (and Floating Diffusion)
    - → higher sensitivity (smaller C) & lower noise (CDS)
    - → ***global shutter*** (allows snapshots)

4T:

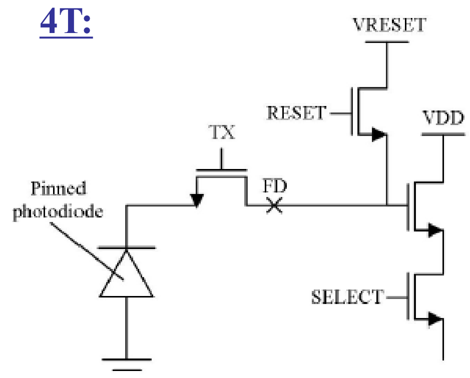

3T:

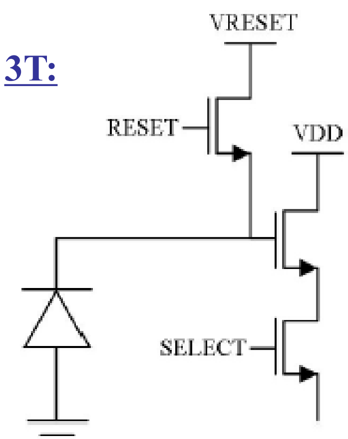

R. Coath et al., Advanced Pixel Architectures for Scientific Image Sensors, 2009

CMOS Working Principle (2)

- CIS structure and readout
  - each pixel (a)
    - → amplified voltage signal
  - pixel-select switch (e, Select Transistor) turned on
    - → outputs amplified voltages of all pixels in selected row (j) to their respective column circuit (h, sample & hold)
    - → slow speed parallel readout
  - column-select switch (g) turned on from left to right
    - → signal voltages of each pixel in row are read out
    - → high speed serial readout
  - repeat operation for all rows from top to bottom

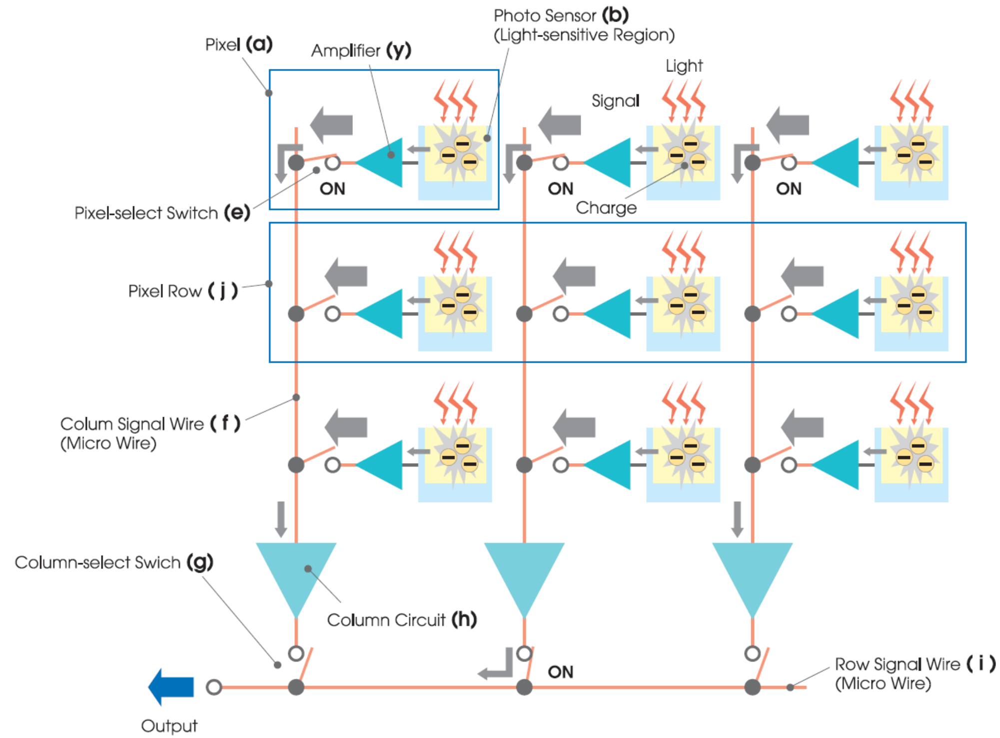

www.sony.com/professional

- consequences
  - voltage transfer
    - → faster than charge transfer in CCDs (~ 100 fps vs. 20 fps)
  - windowing
    - → readout of sub-structures → even faster readout
  - reduced fill factor (amplifier on CIS)
    - → micro-lenses

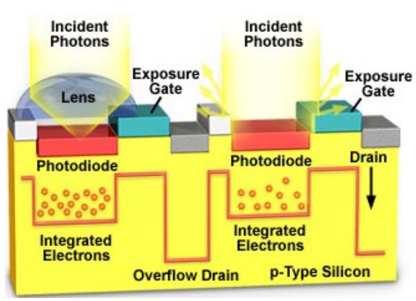

http://micro.magnet.fsu.edu/primer/

Comparison CCD versus CMOS

- mechanisms of CCD and CMOS image sensors

www.sony.com/professional

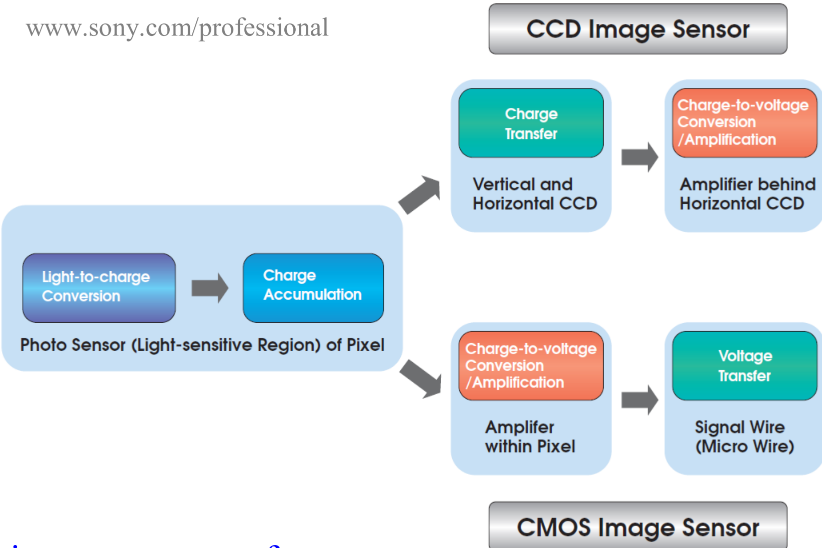

- image sensor performance

Photonics Spectra, Issue January 2001

- responsitivity
- dynamic range
- uniformity
- shuttering
- speed
- windowing
- antiblooming
- biasing & clocking

better image sensor type ???

Sony announced in March 2015 that it was discontinuing its entire line of CCD sensors…

- camera architecture
  - CCD

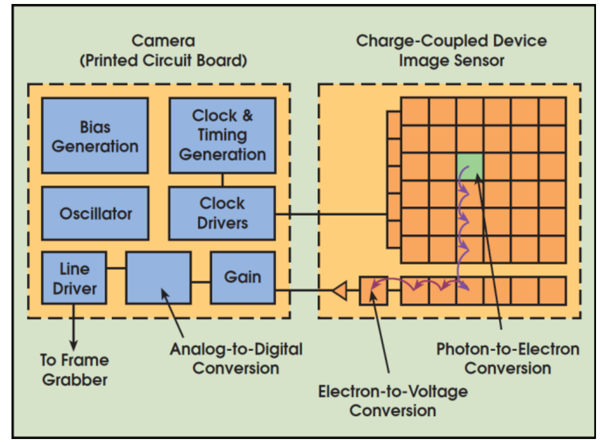

  - CMOS

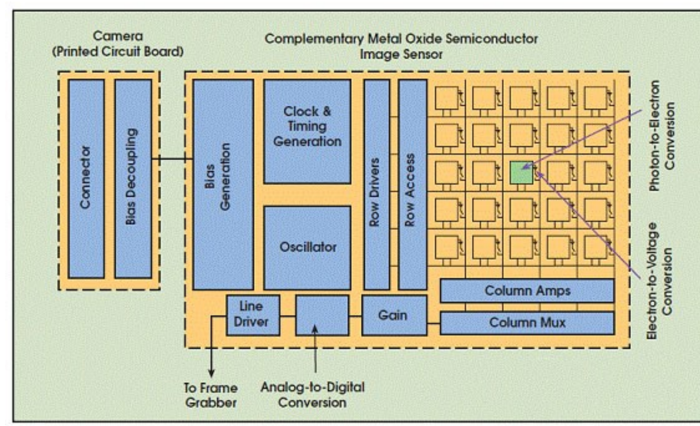

Photonics Spectra, Issue January 2001

Digital Camera Interfaces

- various interfaces in overview

Interface	Cable length	Band width maximum in MB/s.	Multi-camera	Cable costs	„Real-time“	„Plug & Play“
USB 2.0	5m	40	orange	orange	red	green
FireWire	4.5m	64	orange	orange	green	green
GiGE VISION	100 m	100	green	green	orange	orange
USB3 VISION	8 m	350	orange	orange	green	green
CAMERA Link	10 m	850	red	red	green	red

Basler White Paper1505, www.baslerweb.com

Testing Camera Performance

1288 EMVA Standard Compliant

- physical camera model

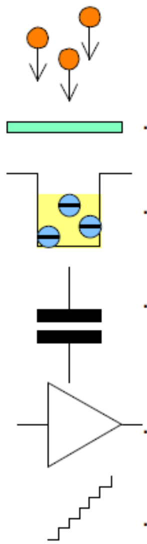

A number of **photons** ...
... hitting a **pixel** during exposure time ...
... creating a number of **electrons** ...
... forming a **charge** which is converted by a **capacitor** to a **voltage** ...
... being **amplified** ...
... and **digitized** ...
42 ... resulting in the **digital gray value**.

- mathematical model of single pixel

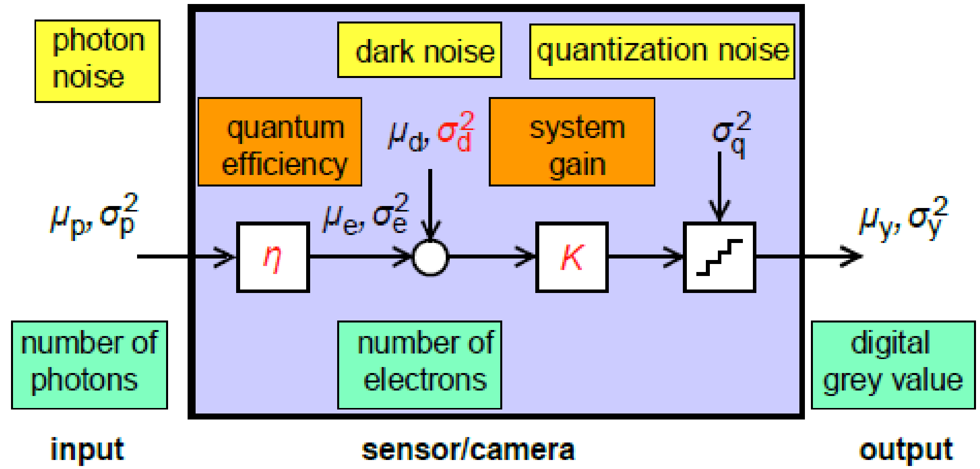

EMVA Standard 1288, Release 3.1, Release Candidate (2012), www.emva.org

- mathematical model: validity
  - amount of photons depend on radiative energy density
  - sensor linearity (valid for λ > 400 nm)
  - noise sources are stationary and white
  - only total quantum efficiency depends on λ
  - only dark current depends on temperature

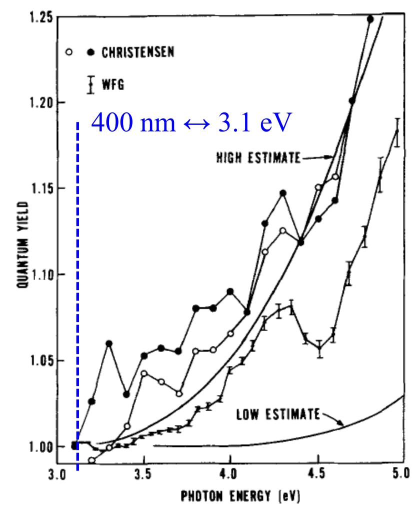

F.J. Wilkinson et al., J. Appl. Phys. **54** (1983) 1172

Photon Transfer Method

- basic assumptions
  - number of photons/electrons: stochastic values

    → charcterization by mean/variance

mean number of photons: $\mu_p = \sigma_p{}^2$

mean number of electrons: $\mu_e = \eta \mu_p$

$\sigma_e{}^2 = \mu_e = \eta \mu_p$

(Poisson distributed)

- CCD output
  - grey value **y**

    → unit DN (digital number)
  - simplification

    → neglect quantization noise σ_q

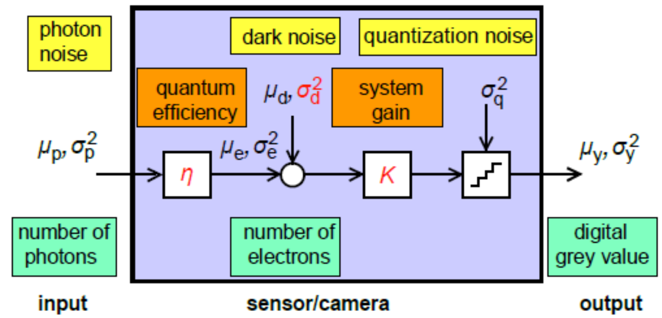

$$\mu_y = K(\mu_e + \mu_d) = K\,\eta\mu_p + \mu_{y,dark}$$

$$\sigma_y{}^2 = K^2(\sigma_e{}^2 + \sigma_d{}^2) = K(\mu_y - \mu_{y,dark}) + \sigma_{y,dark}{}^2$$

Photon Transfer Method

- measurement
  - μ_y, $\sigma_y{}^2$ as function of μ_p

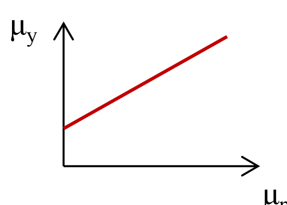

slope: $K\eta$

offset: $\mu_{y,dark}$

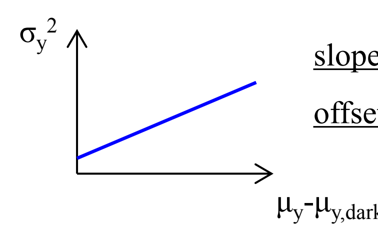

slope: K

offset: $\sigma_{y,dark}{}^2$

PT Measurements

- CCD under test → Basler Aviator avA1600-gm
  - for each exposure time (μ_p): take 10 images
  - select ROI: 50 x 50 pixels
    - → determine mean gray value and noise variance: μ_y, σ_y^2
- analysis

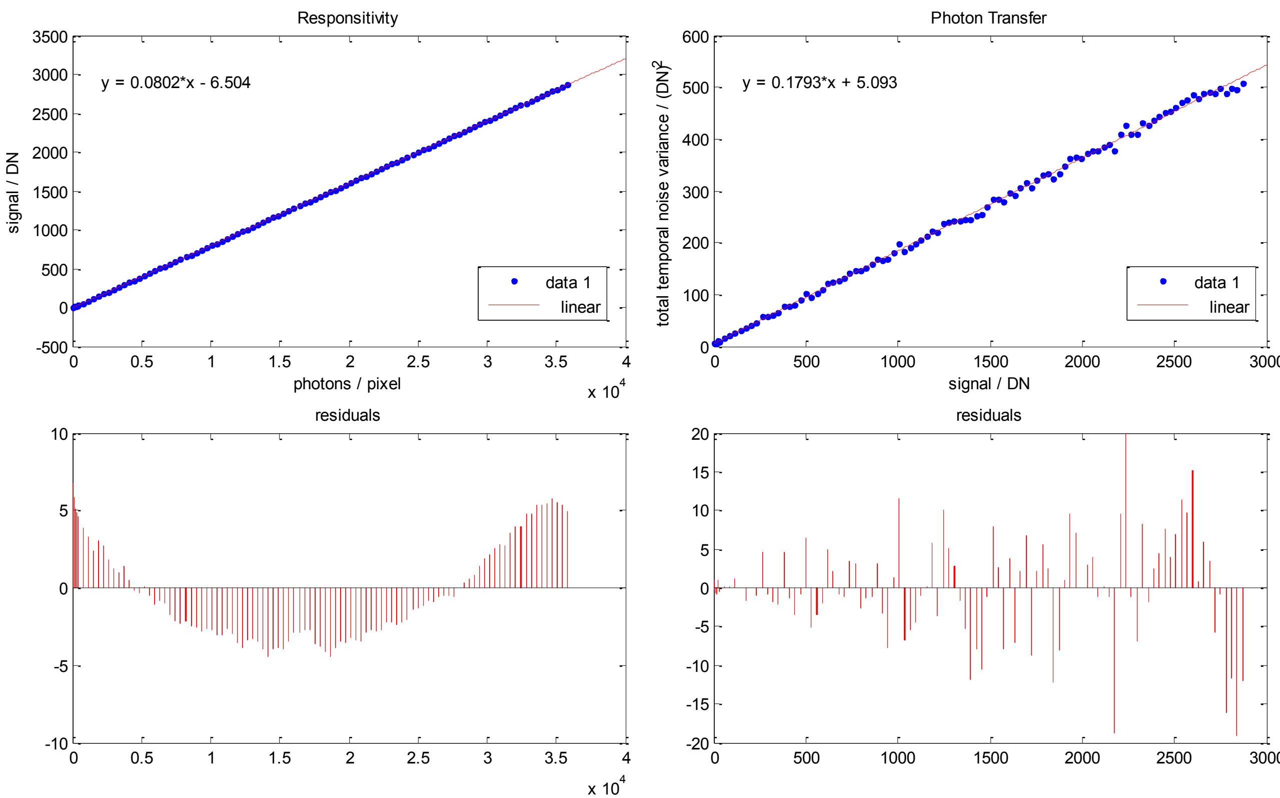

- results
  - overall system gain
    - $K = 0.1793$ DN/e$^-$
    - → $K^{-1} = 5.6$ e$^-$/DN
  - QE @ 470nm
    - $K\eta = 0.0802$
    - → $\eta = 0.447$
  - dark noise
    - $\sigma^2_{y,dark} = (5.093\ \text{DN})^2$
    - → $\sigma_d = 12.6$ e$^-$
  - EMVA 1288 data sheet

Item	Symbol	Typ.[1]	Unit
Temporal Noise Parameters			
Total Quantum Efficiency (QE)	η	40	%
Inverse of Overall System Gain	$\frac{1}{K}$	4.8	$\frac{e^-}{DN}$
Temporal Dark Noise	σ_{d_0}	11	e^-
Saturation Capacity	$\mu_{e.sat}$	18500	e^-

www.baslerweb.com (QE @ 545 nm)

Signal-to-Noise Ratio

- measure for signal quality
  - usually in logarithmic representation

$$SNR_y(\mu_p) = \frac{\mu_y - \mu_{y,dark}}{\sigma_y} = \frac{\eta\mu_p}{\sqrt{\eta\mu_p + {\sigma_d}^2}}$$

$$\Rightarrow \quad ld(SNR_y) = ld(\eta) + ld(\mu_p) - \tfrac{1}{2}\, ld(\eta\mu_p + {\sigma_d}^2)$$

  - ideal sensor: $\eta = 1, \sigma_d = 0$

$ld(SNR_y) = \tfrac{1}{2}\, ld(\mu_p)$ → pure shot noise from photons, i.e. $SNR_y = \sqrt{\mu_p}$

- limiting cases
  - shot noise dominated: $\eta\mu_p \gg {\sigma_d}^2$

$$ld(SNR_y) = \tfrac{1}{2}\, ld(\mu_p) + \tfrac{1}{2} ld(\eta)$$

  - dark noise dominated: $\eta\mu_p \ll {\sigma_d}^2$

$$ld(SNR_y) = ld(\mu_p) + ld(\eta/\sigma_d)$$

  - intersection with $SNR_y = 1$:

courtesy F. Dierks (Basler AG)

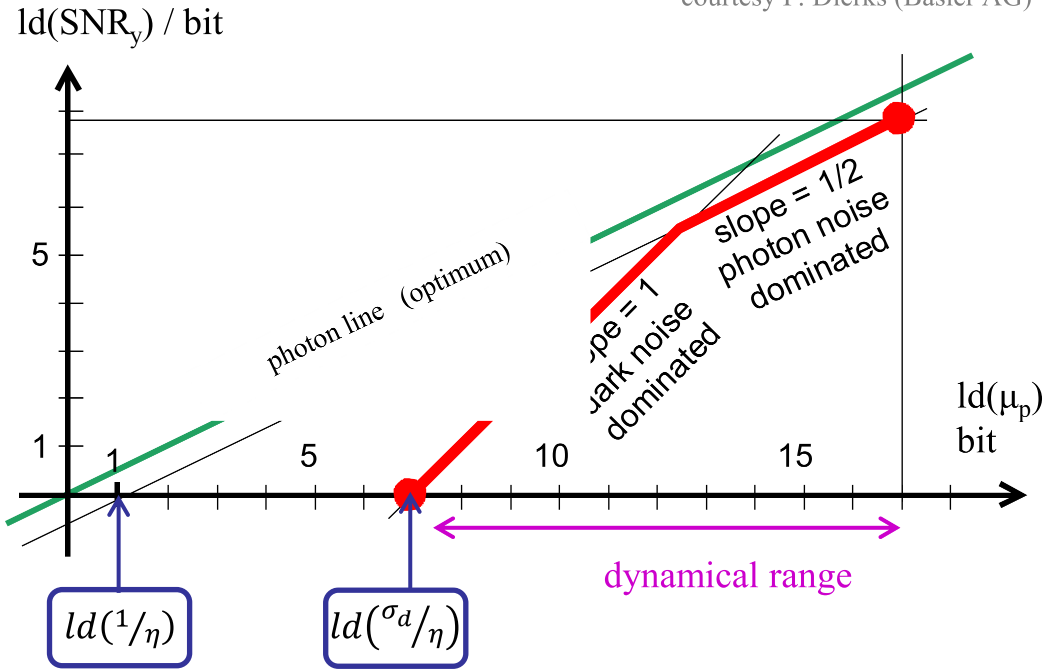

Signal-to-Noise Analysis

- CCD under test → Basler Aviator avA1600-gm
  - same data set as before
- QE (η) and dark noise (σ_d)
  - from intersection with ld(SNR) axis → SNR = 1

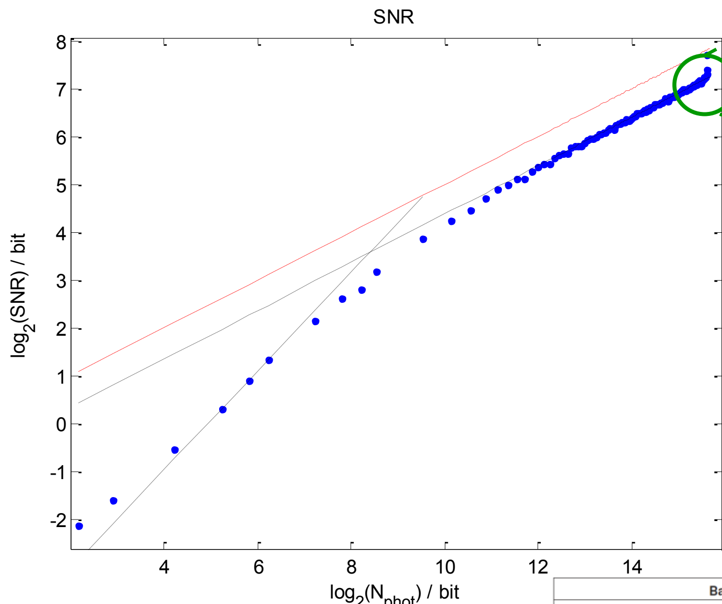

- dynamical range (DR) and saturation (ST)

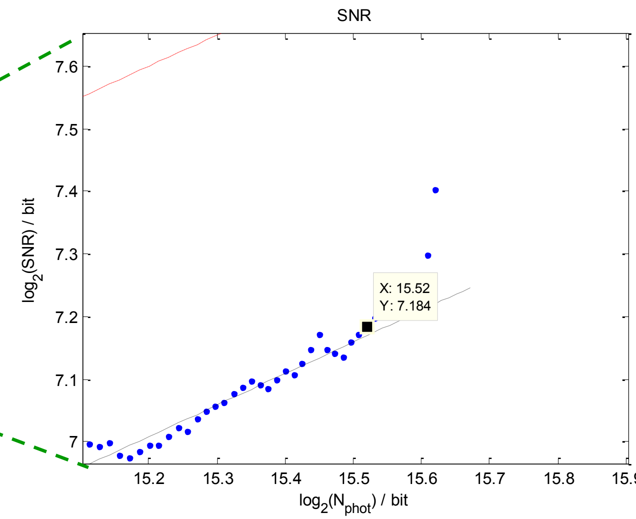

- minimum number of photons

$$\mu_{p,min} = \sigma_d / \eta = 30.6$$

- maximum number of photons

$$\mu_{p,sat} = 2^{15.52} = 46988$$

$\eta = 0.40$

$\sigma_d = 12.2\ e^-$

www.baslerweb.com

Basler avA1600-50gm				
Item	Symbol	Typ.[1]	Unit	Remarks
Temporal Noise Parameters				
Total Quantum Efficiency (QE)	η	40	%	$\lambda = 545\,nm$
Inverse of Overall System Gain	$\frac{1}{K}$	4.8	$\frac{e^-}{DN}$	
Temporal Dark Noise	σ_{d_0}	11	e^-	
Saturation Capacity	$\mu_{e.sat}$	18500	e^-	
Derived Parameters				
Absolute Sensitivity Threshold	$\mu_{p.min}$	28	$p^\sim$	$\lambda = 545\,nm$
Dynamic Range	$DYN_{out.bit}$	10.7	bit	
Maximum SNR	$SNR_{y.max.bit}$	7.1	bit	
	$SNR_{y.max.dB}$	42.7	dB	

DR = 1535 = 63.7 dB = 10.6 bit

ST = $\mu_{p,sat}\,\eta$ = 18800 e^-